Title

Investigating the effect of particle size on pulmonary surfactant phase behavior.

Journal

Biophysical Journal, 107(7)

Authors

Kodama, Akihisa

Kuo, Chin-Chang

Boatwright, Thomas

et al.

Publication Date

2014-10-07

DOI

10.1016/j.bpj.2014.08.010

Peer reviewed

Article

Investigating the Effect of Particle Size on Pulmonary Surfactant Phase Behavior

Akihisa T. Kodama,[1] Chin-Chang Kuo,[1] Thomas Boatwright,[1] and Michael Dennin[1,*]
[1]Department of Physics & Astronomy, University of California, Irvine, California

ABSTRACT We study the impact of the addition of particles of a range of sizes on the phase transition behavior of lung surfactant under compression. Charged particles ranging from micro- to nanoscale are deposited on lung surfactant films in a Langmuir trough. Surface area versus surface pressure isotherms and fluorescent microscope observations are utilized to determine changes in the phase transition behavior. We find that the deposition of particles close to 20 nm in diameter significantly impacts the coexistence of the liquid-condensed phase and liquid-expanded phase. This includes morphological changes of the liquid-condensed domains and the elimination of the squeeze-out phase in isotherms. Finally, a drastic increase of the domain fraction of the liquid-condensed phase can be observed for the deposition of 20-nm particles. As the particle size is increased, we observe a return to normal phase behavior. The net result is the observation of a critical particle size that may impact the functionality of the lung surfactant during respiration.

INTRODUCTION

The process of respiration is of vital importance to sustain life in most land-based animals. In humans, gas exchange occurs through the alveoli in the lungs and is fundamentally a dynamic process. The alveoli expand and compress during inhaling and exhaling, and the surface is covered by water-based alveolar fluid. To protect the alveoli from completely emptying of air and filling with fluid, surfactant films, produced by the alveolar cells, minimize surface tension of the alveolar fluid-air interface. In addition, the reduction of surface tension by the lung surfactant minimizes the work required for breathing (1–3). A lack of lung surfactant can have adverse effects on our health. A common instance is with premature infants. They may develop a condition known as neonatal respiratory distress syndrome (NRDS), which is characterized by insufficient production of lung surfactant from their alveolar cells. Administering replacement surfactant to the infant has greatly reduced the mortality rate from NRDS (4). Therefore, understanding interaction of the lung surfactant layer under compression and expansion is important for a full understanding of the lung function.

A relatively good model system for studying dynamics of lung surfactant is the surfactant films at the air-water interface in a Langmuir trough. Surfactant films consist of layers of molecules with a hydrophilic head and hydrophobic tail (5). Lung surfactant is composed of several different components (3). Its main constituent is an amphiphilic phospholipid known as DPPC (dipalmitoylphosphatidylcholine) (1,3,6). This saturated phospholipid allows the lung surfactant to reach a high surface pressure and stabilize the alveoli at the end of expiration. The remaining lipids are mainly unsaturated, such as POPC (phosphatidylcholine), POPG (phosphatidylglycerol), and POPI (phosphatidylinositol). Other important components of lung surfactant include several associated surfactant proteins (SP). In previous works, the associated proteins are shown to be related to the mechanical properties of the lung surfactant (6–18). SP-B aids surfactant films folding by enhancing flexibility while preventing material loss to the subphase. On the other hand, SP-C is responsible for maintaining the fluidity of the surfactant films and separating areas of solid-phase lipids up to films collapse (7). This combination of molecules and proteins maintains the functionality of lung surfactant in the alveoli.

During the compression of the surface area, pulmonary surfactant is known to go through several phases. One general method to study the phase transition is via surface area versus surface pressure isotherm measurements (1,2,5,19). In its expanded state, the surfactants form a liquid-expanded phase. In this state, the tails of the molecules are disordered and associate to each other instead of contacting with the water surface. With further compression, the isotherm exhibits a coexistence between the liquid-expanded (LE) and liquid-condensed (LC) phases. In the LC phase, the tails of the molecules interact with each other and align such that they point in the same direction. Moreover, at ~40 mN/m of the surface pressure, the coexistence phase signifies a plateau behavior. The plateau is also known as the squeeze-out plateau because unsaturated lipids in Survanta (Abbvie, North Chicago, IL) forms reservoirs and multilayer structures under the interface (6,10,20). By further

Submitted January 29, 2014, and accepted for publication August 6, 2014.
*Correspondence: mdennin@uci.edu
Akihisa T. Kodama and Chin-Chang Kuo contributed equally to this work.
Editor: Ka Yee Lee.

0006-3495/14/10/1573/9 $2.00
http://dx.doi.org/10.1016/j.bpj.2014.08.010

decreasing the surface area, the isotherm rises as the LC phase becomes more prevalent. At ~68 mN/m of the surface pressure, the lung surfactant reaches the collapse region (2,21–24). A giant fold phenomenon can be observed in this system (1,7). A significant question is how this phase behavior is impacted by the presence of particulate matter.

Particulate matter can result from a variety of sources including dust, pollen, pollution, and dander. The impact of particles into the biological systems depends on diverse properties such as materials, surface conditions, particle sizes, surface area, and particle shapes (25–31). The effect of the deposition of nanoparticles on the Langmuir films has been studied in various systems, including phospholipid monolayers, lung surfactant, and model lung surfactant (32–40). In particular, ultrafine particles with diameters $<$100 nm can be transported to the alveoli (39,41,42). It has been shown that the addition of 15 nm gold particles drastically reduced the surface activity of the system (39). Studies indicate that a majority of particles remain on the alveolar surface after 24 h (43–45).

This can cause a buildup of fine particulate matter in the lung surfactant of people who live or work in heavily polluted areas and may have an advanced impact on the functionality of the alveoli (46). One potential consequence of these particles is a disruption of the phase behavior. Further, the interaction between the negatively charged carboxylate-modified microspheres with a particle size of 200 nm and monolayers of DPPC has been studied. This work shows that the deposition of particles affects the isotherm behavior by increasing the hysteresis area between the compression and expansion cycles (37). In addition, hydrophobic polyorganosiloxane nanoparticles with sizes of 136 and 12 nm were studied in phospholipid films with the addition of SPs. This work shows that the size of nanoparticles is a critical factor responsible for causing severe structural and functional damage to the model lung surfactant films (40). Further, significant amounts of nanoparticles are retained at the interface and are released slowly into the aqueous subphase during compression and expansion cycles (47). Thus, understanding how particles of different sizes impact phase transitions in surfactant layers is an important issue.

In this article we investigate the impact of particle size on the phase behavior of the lung surfactant. We focus on particles in the range from 1.0 μm to 20 nm. The rest of the article is organized into several sections. Materials and Methods outlines the experimental details and the procedures for the preparation of the surfactant films and particle solutions. In addition, we illustrate the experimental results for the surface area versus surface pressure isotherm measurements with the accompanied fluorescent microscope observation. In the Discussion, we propose a potential schematic for the impact of the particle size effect to the phase transition behavior in the lung surfactant system.

MATERIALS AND METHODS

We use Survanta (Abbvie) purchased from Abbott Nutrition (Columbus, OH) to produce lung surfactant films. The product Survanta (generic name: beractant) is bovine lung surfactant that is clinically used to treat premature infants with NRDS (2). Compared to the lavaged calf-lung surfactant, Survanta has fewer surfactant proteins (i.e., decreased SP-B) due to the extraction of hydrophobic solvents performed during commercial processing. The initial concentration of phospholipids in Survanta is 25 mg/mL. To ensure the even distribution of the Survanta films, we dilute the concentration of phospholipids in Survanta to 1 mg/mL with a prepared buffer solution without additional purification. This gives a DPPC concentration of ~1.16×10^{-3} M. The same buffer solution is used as the aqueous subphase for all the experiments (2). The water used in the buffer solution is filtered through a Milli-Q system (Millipore, Billerica, MA) with a measured resistivity of 18.2 MΩ. The buffer solution is composed of 150 mM NaCl, 5.0 mM CaCl, and 0.2 mM $NaHCO_3$. We ensure the pH value of the buffer solution is between 6.9 and 7.3 before conducting experiments.

Microspheres are spherical particles formed from an amorphous polymer. The carboxylate-modified microspheres create a charged surface around the particles. In our experiments, we use microspheres made by polystyrene, which has the density of 1.055 g/cm^3. Different sizes of red fluorescent carboxylate-modified polystyrene microspheres are obtained from Invitrogen (Carlsbad, CA). The nominal particle diameters are 1.0, 0.5, and 0.1 μm, and 40 and 20 nm. Additional particles of 30 nm are obtained from Sigma-Aldrich (St. Louis, MO). The details of the actual particle size, particle charge, specific surface area, and surface charge density are exhibited in Table 1. All particle solutions are diluted to 1% solids by the addition of Milli-Q water (Millipore) to the original solution. The particle solutions are sonicated thoroughly before conducting experiments. A fluorescent tag of NBD C12-HPC (1-palmitoyl-2-[12[(7-nitro-2-1, 3-benzoxadiazol-4-yl) amino] dodecanoyl]-*sn*-glycero-3-phosphocholine) obtained from Avanti Polar Lipids (Alabaster, AL) is used to visualize the domain structure during phase coexistence. The fluorescent tag powder is dissolved in a 3:1 chloroform-methanol solution such that the final concentration of the fluorescent tag is 0.1 mg/mL.

Two experimental methods are utilized to study the lung surfactant films with the deposition of nanoparticles:

Method 1

Our initial studies used standard methods of putting the florescent tag directly into the aqueous mixture of Survanta solution so that the tag and Survanta are placed on the water surface simultaneously. Using this

TABLE 1 The actual particle size, particle charge, specific surface area, and surface charge density of carboxylate-modified polystyrene microspheres

Nominal particle size	1.0 μm	0.5 μm	0.1 μm	40 nm	30 nm	20 nm
Average actual size	1.1 μm	0.49 μm	0.109 μm	0.045 μm	0.032 μm	0.024 μm
Charge (milliequivalents/g)	0.0175	0.315	0.3092	0.725	0.07	0.7512
Specific surface area (cm^2/g)	5.2×10^4	1.2×10^5	5.2×10^5	1.3×10^6	1.8×10^6	2.4×10^6
Charge density (milliequivalents/cm^2)	3.4×10^{-7}	2.6×10^{-6}	5.9×10^{-7}	5.6×10^{-7}	3.9×10^{-8}	3.1×10^{-7}

Specific surface areas for 30-nm particles are estimated by average actual sizes.

method, we observe bright dots on the surface at the surface pressure of ≈40–45 mN/m, consistent with previous studies. However, these structures inhibit the quantitative analysis of the domain structure. In addition, for our studies, we utilize a number of compression and expansion cycles before the cycles of interest for measurement in order to fully relax the system. In this case, we find that the intensity of the florescence significantly decays. Therefore, to clearly observe the domain structure, a slightly different procedure is utilized to observe and record the images of the lung surfactant films. After two cycles of compression and expansion, 15 μL of the tag solution is deposited on the surface by the same method with the deposition of lung surfactant and particles solutions. At this point, the experiment is conducted in the dark room to preserve the fluorescence of the tag. Another 15 min elapsed before an additional compression and expansion cycle is applied to ensure the even distribution of the fluorescent tag. The images of the fourth compression cycle are observed and recorded at different surface pressures. We do not find any significant difference in the isotherm measurement with or without the presence of fluorescent tag solution. The ratio between the LC and LE phase is measured by the ratio of the binary image processed by a MATLAB program (The MathWorks, Natick, MA).

Method 2

Surface area versus surface pressure isotherms at constant temperature are measured in a Langmuir trough (Nima model No. 102M; Biolin Scientific, Stockholm, Sweden). The surface pressure is measured by a tensiometer via the standard Wilhelmy method. The compression of the surface area is from 79.0 to 18.0 cm^2 with a compression speed of 15 cm^2/s. The temperature of the aqueous subphase is controlled to be 37°C by a water-cycling heating system. To conduct the measurement, we fill the Langmuir trough with 50-mL buffer solution. Then we deposit 150 μL of the Survanta solution by evenly contacting and extracting droplets of the solution from the tip of a syringe on the liquid surface. We wait for 15 min to allow the surfactant to spread homogeneously over the surface. Afterwards, particles are deposited in a similar process as used for the surfactant with another 15-min pause before the measurement of five compression and expansion cycles. The domain structure and deposited particles are observed by a fluorescence microscope (model No. BX60MF5; Olympus, Melville, NY) with a charge-coupled device camera.

RESULTS

Surface pressure versus surface area isotherms

A typical isotherm measurement of pure lung surfactant under compression and expansion for five cycles is shown in Fig. 1. The Survanta is deposited at the air-liquid interface by the process described in Materials and Methods. The surface area versus surface pressure isotherm of pure lung surfactant is measured at 37°C, which is approximately normal physiological temperature. Several different phases of lung surfactant are observed in the measurement. Starting from a surface pressure of ≈15 mN/m, a small increase of the surface pressure under compression can be observed. As the surface area decreases, the slope of the isotherm becomes steeper, indicating the onset of LC phase formation. Due to the multicomponent surfactant, it is standard to only see the change in slope (2). This is in contrast to the pure DPPC system in which one observes a plateau during the LC/LE coexistence. With further compression, a plateau region is reached, which is associated with the monolayer-to-multilayer transition that is controlled by the surfactant proteins (i.e., the squeeze-out plateau) (6,10). Upon further compression, the increase of the isotherm slope corresponds to the LC phase dominating the lung-surfactant films.

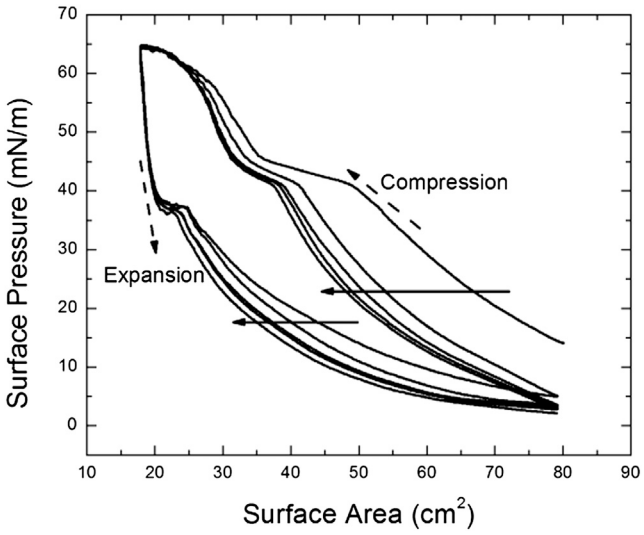

FIGURE 1 Isotherm of pure lung surfactant over five compression and expansion cycles. (*Solid arrows*) Progression isotherm measurements from the first to the fifth cycle. (*Dashed arrows*) Directions of compression and expansion. Several phase transitions occur under compression. The LE to LC-LE coexistence transition corresponds to the observed change in slope ~15 mN/m. Under further compression, the squeeze-out plateau is observed when the surface pressure is ~42 mN/m. At the surface pressure of ~65 mN/m, we observe an LC phase collapse. An elastic stretching is observed at the surface pressure of ~37 mN/m under expansion.

Beyond a surface pressure of 65–68 mN/m, the film collapses, and the formation of giant folds occurs on the surface (1,7). Under expansion, the isotherms show a drastic decrease of the surface pressure followed by a slight elastic stretch when the surface pressure is ~37 mN/m. This elastic-stretch behavior is related to the recovery of films from its collapse and folding at the high surface pressure (49). Consecutive compression and expansion cycles are indicated as arrows in Fig. 1. A significant shift between the first and second compressions exhibits a large amount of material loss from the surface when the film collapses during the first compression. Furthermore, consistent shifts of the isotherms can be observed in the stabilized surfactant films after the first compression. The phase behavior is identical across the multiple compression and expansion cycles.

We utilized the isotherm measurements of the lung surfactant with the deposition of particles to study the impact of particles size on the phase behavior. We apply five compression and expansion cycles to the surfactant films and the comparison of the isotherms for the particles measuring (*a*) 20 nm, (*b*) 40 nm, and (*c*) 0.5 μm, as shown in Fig. 2. The arrows in the figures indicate the order of the isotherm shift from the first to fifth compression and expansion cycles. For all particle sizes, the first compression illustrates phase behavior similar to the pure lung surfactant. At the third

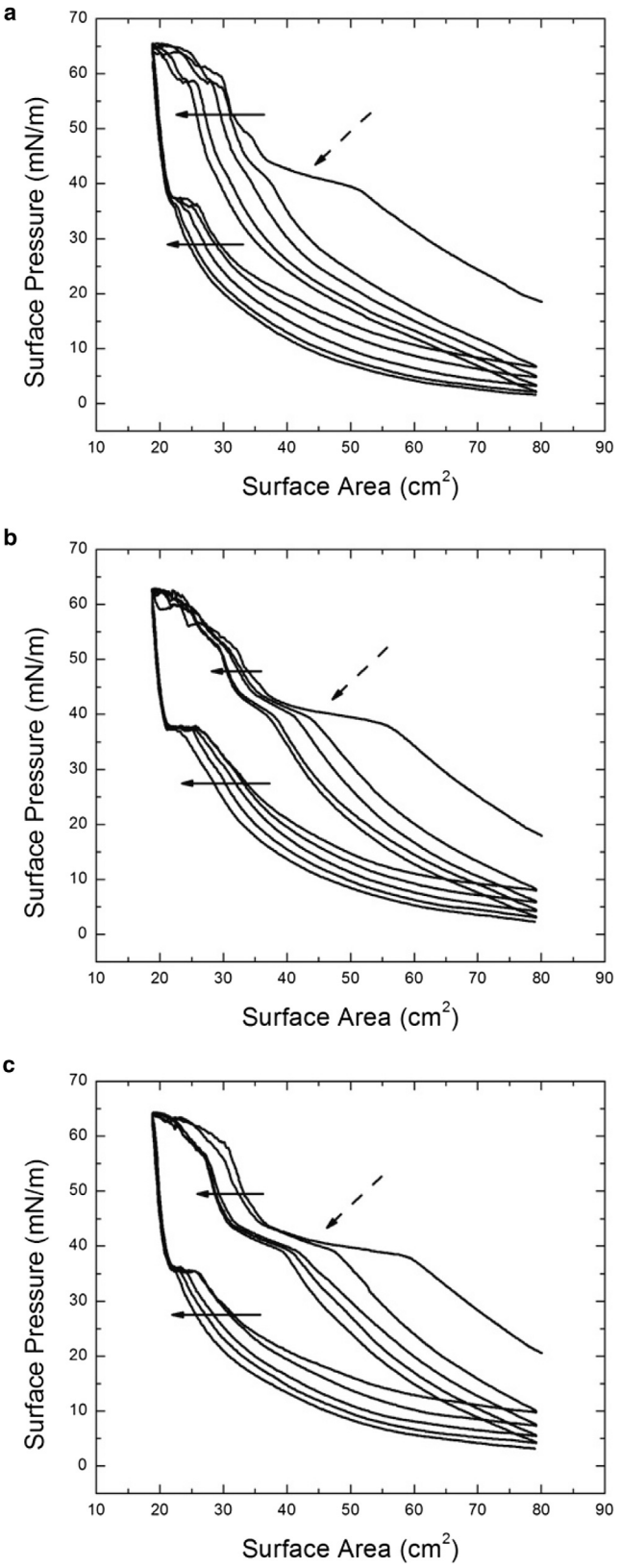

FIGURE 2 The surface pressure versus the surface area isotherm measurements of the lung surfactant with various sizes of particles. Three different sizes of particles of (*a*) 20 nm, (*b*) 40 nm, and (*c*) 0.5 μm are shown for five consecutive compression and expansion cycles. (*Solid arrows*) Continuous shifting of isotherms from the first to fifth cycles. (*Dashed arrows*) Observed squeeze-out plateau. During the first compression, there is no significant change for the phase behavior for the surfactant films with deposited particles for all three sizes. After the third compression, the squeeze-out plateau vanishes for the surfactant films with 20-nm particles; whereas the surfactant films in the presence of other particle sizes behave similarly to the pure lung surfactant without the deposition of particles.

compression, a change in phase behavior is observed in the presence of 20-nm particles. The most dramatic feature is the loss of the squeeze-out plateau. Instead, a constant increase in the slope of the surface pressure from the LE-LC coexistence phase to the LC phase under the compression is observed. This behavior is repeated in all further compression cycles. For all particle sizes >20 nm, we do not observe the annihilation of the squeeze-out plateau. This indicates a critical particle size close to 20 nm that impacts the phase transition behavior of the lung surfactant.

With the deposition of 20-nm particles on the surfactant films, the annihilation of the squeeze-out plateau occurs with repeated compression cycles. We also vary the initial concentrations of the 20-nm particle solutions. Fig. 3 *a* shows the isotherms of the lung surfactant with 20-nm particles for 1, 0.5, and 0.33% solids on the fifth compression. Changes in the horizontal shifts for each particle concentration are due to the differences of the material loss in each individual measurement. We observe that a significant annihilation of the squeeze-out plateau occurs for the 1 and 0.5% solid solutions on the fifth compression whereas the deposition of 0.33% solid solution does not cause a significant difference. This suggests that the effect requires a minimum number of particles within the critical size range to impact the phase behavior.

In addition, the isotherms of 20-, 30-, and 40-nm particle solutions with 1% solid at the fifth cycle are exhibited in Fig. 3 *b*. The phase behavior of the 30-nm particle is intermediate between the 20- and 40-nm particles, particularly in terms of the size of the plateau as indicated by the arrow. To determine the impact of the total surface area of the particles on the phase behavior, we use 20-, 40-, and 0.1-μm particle solutions with adjusted concentrations. Based on the solid weight concentration of 20-nm particles solution, we use two-times the 40-nm particles solution and five-times the 0.1-μm particles solution to deposit a similar total-particle-surface area. The comparison between the surfactant films with the adjusted amount of 20-nm, 40-nm, and 0.1-μm particles at the fifth compression is shown in Fig. 3 *c*. In both the surfactant films with 40-nm and 0.1-μm particles, the plateau exists regardless of the change of the depositing amounts. This suggests that only the 20-nm particles interfere with the phase transition of the lung surfactant.

LC domain observation

Observations of the particle impact on domain morphology using a fluorescence microscope are shown in Fig. 4. The

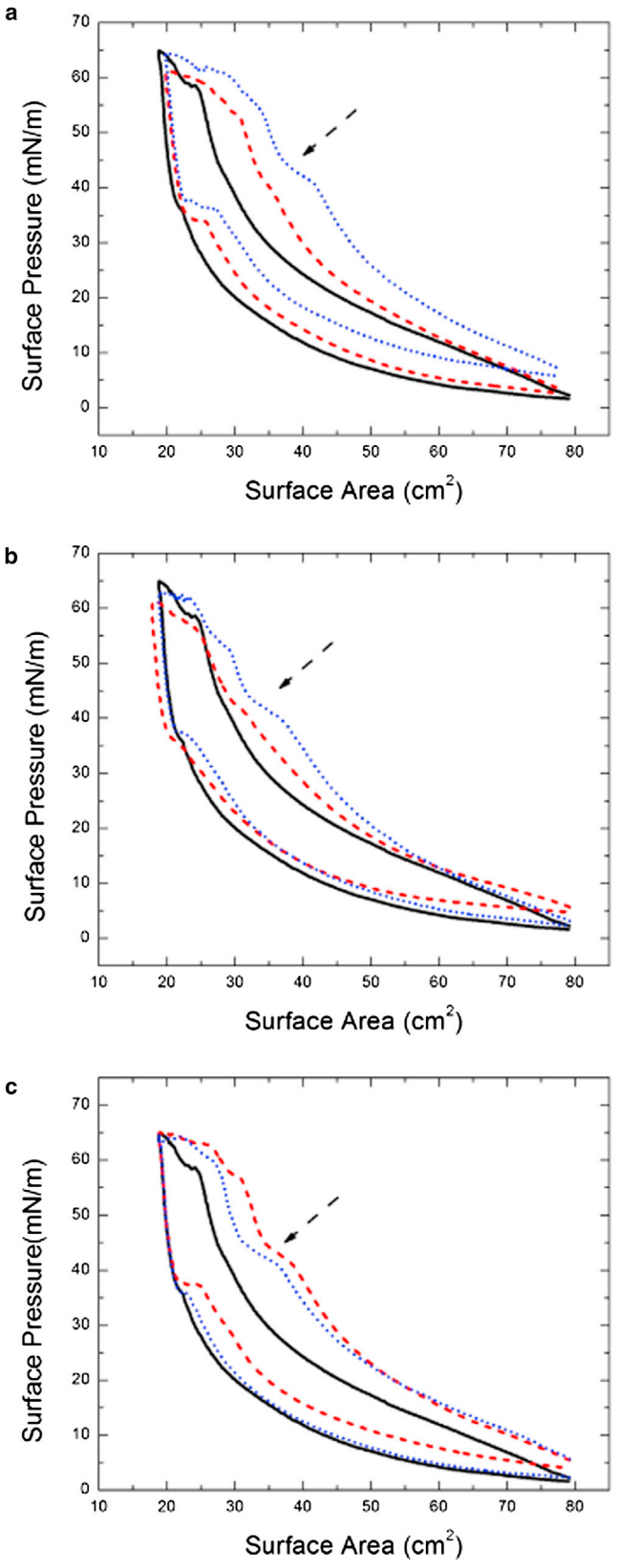

FIGURE 3 The isotherm measurements of the lung surfactant with different depositions of particles at the fifth cycle. (*Dashed arrows*) Observed squeeze-out plateau. (*a*) The isotherms of lung surfactant with various amounts of the 20-nm particle solutions. We deposit three different solid concentrations for the 20-nm particles solutions: 1% solid (*black solid*), 0.5% solid (*red dashed*), and 0.33% solid (*blue dotted*). Only the 1% particles solution exhibits a complete removal of the squeeze-out plateau on the fifth compression. This indicates a threshold for the particle concentration necessary to cause the effect. (*b*) The isotherms of lung surfactant with different sizes of 1% solid particle solutions: 20 nm (*black solid*), 30 nm (*red dashed*), and 40 nm (*blue dotted*). The isotherm of 30 nm is intermediate between the deposition of 20 nm and 40 nm particles. (*c*) The isotherms of lung surfactant with different sizes and amounts of particles on the fifth compression and expansion cycle. In this case, the volume of the solutions of 20 nm (*black solid*), 40 nm (*red dashed*), and 0.1 μm (*blue dotted*) are adjusted to give similar total surface area of the particles. The results show a significant particle size effect only for 20-nm particles, indicating that total surface area of deposited particles is not relevant. To see this figure in color, go online.

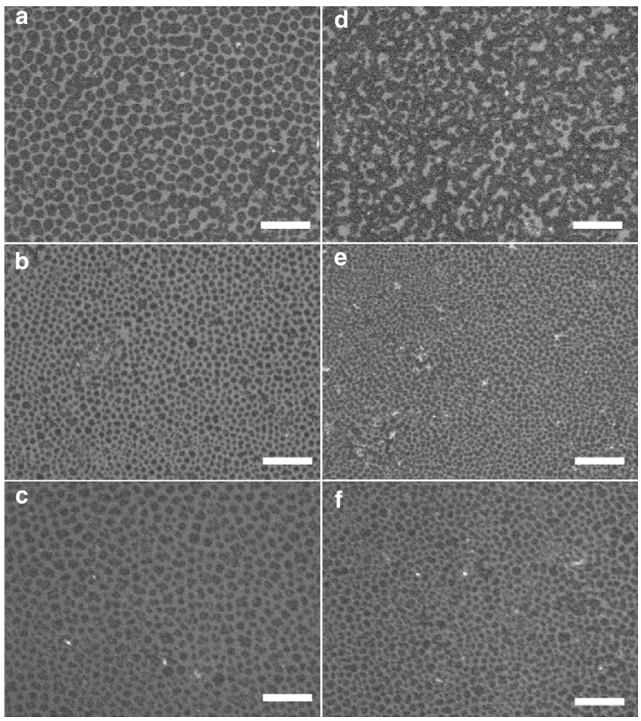

FIGURE 4 The fluorescent microscope images of the lung surfactant films with the deposition of particles at different surface pressure. The images of different particles are shown in panels *a* and *d* for 20 nm, panels *b* and *e* for 40 nm, and panels *c* and *f* for pure lung surfactant. The deposition volume is 50 μL for each particle size. The surface pressures for the images are 34 mN/m for panels *a–c* and 42 mN/m for *d–f*. The scale bars in images are 130 μm. A small ratio of the fluorescent tag is deposited on the lung surfactant for the observation of the domain structure. (*Bright* and *dark regions*) LC domain and LE liquid phase, respectively.

images are taken at surface pressures of 34 mN/m (Fig. 4, *a–c*) and 42 mN/m (Fig. 4, *d–f*), which correspond to the observation of the LC-LE coexistence phase and the squeeze-out plateau under compression. Two different particle sizes of 20 nm (Fig. 4, *a* and *d*) and 40 nm (Fig. 4, *b* and *e*) are used as a comparison with the pure lung surfactant (Fig. 4, *c* and *f*). The observation of the morphology change

of DPPC domains in the LC phase has been utilized to study various DPPC and lung surfactant systems (2,36–38,50–53). In our experiment, we observe the previously reported behavior that the LC solidlike domains appear on the surface when it reaches the LC-LE coexistence phase (Fig. 4 *c*). Further compression toward the liquid squeeze-out plateau results in no significant change for the domain structure (Fig. 4 *f*). This corresponds to the formation of the reservoir underneath the LE phase. A slight difference of the domain size in Fig. 4, *c* and *f*, is due to the strong localized domain size fluctuation in different locations on the surface.

For the deposition of 20- and 40-nm particles on the surfactant films, we observe two different behaviors. For 40-nm particles, we find similar behavior to the pure lung surfactant. The domain structure does not have any significant change at the surface pressures of 34 and 42 mN/m (Fig. 4, *b* and *e*). However, a significant change of the domain structure can be observed with the deposition of 20-nm particles on the surfactant films. At a surface pressure of 34 mN/m, solidlike LC domains occur that are similar to the other cases (Fig. 4 *a*). When the surface pressure rises toward 42 mN/m under compression, the LC domains grow and start to coalesce to form a networklike structure (Fig. 4 *b*). This indicates that the 20-nm particles are most likely impacting the squeeze-out dynamics, but particles of 40 nm or larger do not have a significant effect on this process. This is consistent with the factor that only the deposition of the 20-nm particles causes changes in isotherm measurements.

We are able to quantify the impact on domain formation by measuring the LC domain fraction as a function of the surface pressure. Results for the different sizes of particles are shown in Fig. 5. We focus on surface pressures ranging from 30 to 42 mN/m to capture impact on the squeeze-out phase. Each point corresponds to the average of 10 random binary images processed to detect the LC domain fraction. To compare the increase of the LC fraction, we normalize the data to the value at the surface pressure of 30 mN/m for each size particle to account for background variation in fluorescence. The result shows a gradual increase of the LC fraction, except for the surfactant films with 20-nm particles. In this case, the LC domain fraction increases rapidly compared to the other sizes, then plateaus when the normalized LC fraction is close to 0.3. It remains relatively high until 46 mN/m, where all the particle sizes show similar ratios. This result shows a much quicker growth of the LC domain in the absence of the squeeze-out plateau for the deposition of 20-nm particles.

To further examine the interaction between deposited particles and LC domains, we compare the images of the LC domain to the deposited particles in the same area. The images of the LC domains and the fluorescent particles are observed by fluorescence microscope with different optical

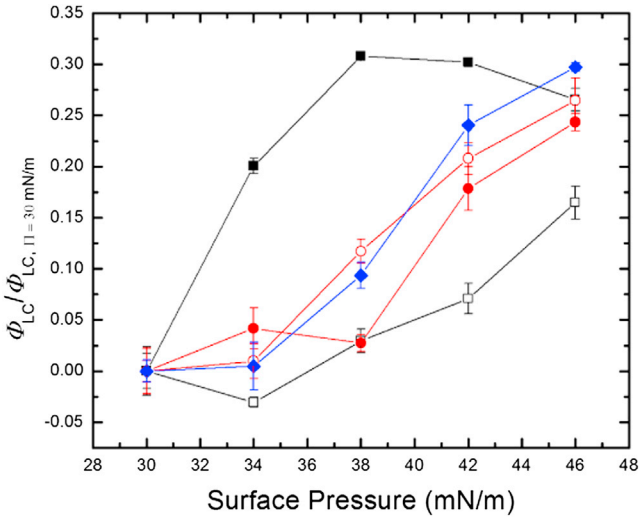

FIGURE 5 The normalized LC domain area fraction as a function of surface pressure. The LC domain area fraction is defined by the ratio between the LC area and the total surface area. The symbols in the plot indicate pure lung surfactant (*open black square*), the lung surfactant with the particles of 20 nm (*solid black square*), 40 nm (*solid red circle*), 0.1 μm (*open red circle*), and 0.5 μm (*solid blue diamond*). The surface pressure ranges from 30 to 42 mN/m and the LC domain area fraction is normalized to the fraction at the surface pressure of 30 mN/m. The deposition of 20-nm particles is seen to cause a rapid growth of the LC domain compared to the other particle sizes and pure lung surfactant. To see this figure in color, go online.

filters for different absorption wave lengths of the fluorescent tag and fluorescent particles. In this observation, we search for the topographic features that can be seen in both channels to confirm the relative positions of LC domains and deposited particles. The overlapping images for the deposition of 20-nm particles and 0.5-μm particles are shown in Fig. 6, *a* and *b*. The LC domains and deposited particles correspond to the green- and red-scale images, respectively. For the deposition of 20-nm particles, we observe that the particles prefer to accumulate inside the LC domain and at the domain boundaries. In contrast, for the deposition of 0.5-μm particles, the domain–particle interaction seems much weaker than the 20-nm particles in which the particles do not show a strong preference to specific locations. It is worth mentioning that we also observe a uniform bright background for the deposition of 20-nm particles with the respective optical filter. This suggests a background of 20-nm particles, which is independent of the LC domain structure and the accumulating particle clumps.

DISCUSSION

From previous research, the formation and structure of the squeeze-out phase provides a unique contribution to the functionality of lung surfactant in respiration (6). The molecules of the LE phase form reservoirs at the

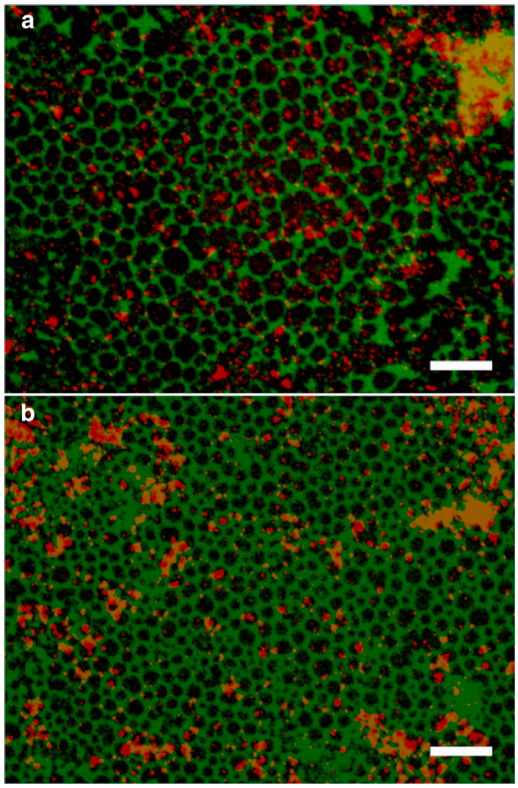

FIGURE 6 Overlapping images of the domain structure and the deposited fluorescent particles. We apply two optical filters to separate the signal from the domain structure and the deposited particles. (*Green scale images*) Domain structure; (*red scale images*) fluorescent particles. The scale bars in images are 130 μm. To compare the domain-particle interaction under compression, two particle sizes of (*a*) 20 nm and (*b*) 0.5 μm are observed at the surface pressure of 34 mN/m. (*Bright dots*) Particles in the images. The scale bars in the images are 130 μm. The relative positions are confirmed by the topographic feature of the impurity particles. To see this figure in color, go online.

squeeze-out plateau region, which provides a lower surface tension under compression and a rapid recovery under expansion (20). The elimination of the squeeze-out plateau is an indication that the formation of reservoirs underneath the LE phase region is prevented. Thus, the surfactant molecules are more likely to form larger LC domains on the surface under compression. This is confirmed by our observation of a rapid increase of the LC domain fraction for case of 20-nm particles. Other research for the lung surfactant at the interface of compressed air bubbles has shown similar behavior. In that case, particles close to 15 nm prevent proper respreading of the layer, but no acknowledged mechanism has been identified (39). Further study is needed to determine whether the mechanism we have identified is relevant to this experiment.

It is interesting to note the connection between our results and previous work focusing on just two different particles sizes and their effects on simplified lung surfactant systems (40). In particular, this work and ours illustrates that one needs to consider not just particle size, but the system of surfactants and the specific phase behavior being studied. For example, the work in Dwivedi et al. (40) reports that 12-nm particles have little effect on the LC/LE phase behavior of pure DPPC, whereas, 0.14-μm particles do impact this phase behavior. When they consider a system of DPPC, DPPG, and a single lung surfactant protein (SP-C), sufficient concentration of 12-nm particles do reduce the plateau. In addition, one interesting feature is that they report sufficient quantities of 0.14 μm increase the plateau, something we did not specifically observe. However, in our studies of a completely different surfactant system, we have shown that nanoparticles impact the collapse of that monolayer only for a specific size window (49). Therefore, comparisons using only a few particle sizes can be misleading if the behavior of interest is due to a specific window of particle sizes, especially if the relevant window is dependent on the details of the monolayer composition. Therefore, further work with a greater variation in particle sizes and the same surfactant systems would be needed for a detailed, quantitative comparison of our observations and those reported in Dwivedi et al. (40).

A general question is whether the surface condition of particles, such as the surface charge density of particles in our experiment, caused the impact to the isotherm behaviors. It is certainly true that one expects surface modifications to exist that will impact the phase behavior. However, our focus is on particles with essentially the same surface properties, so there is only some variation in surface charge (Table 1). In particular, the behavior of the 30-nm particles represents a monotonic change in behavior going from 20 to 40 nm (Fig. 3 *b*), but the corresponding variation in surface charge density is not monotonic (Table 1). This provides the most direct evidence that, for these particles, the change in phase behavior is dominated by the particle size and not the surface properties.

It is known that the total surface area of nanoparticles is associated with the biological activity of the lung surfactant system (25,26,54,55). Therefore, one possible explanation of the observed particle size effect is a purely surface area effect where the surfactant molecules coat the surface of the deposited particles under compression and expansion cycles. However, if this effect was dominant, the annihilation of the squeeze-out plateau should be related to total surface area of particles regardless of the particles' sizes. Our isotherm and optical measurements confirm that 20-nm particles eliminate the squeeze-out plateau of the lung surfactant, whereas particles with the sizes $>$40 nm do not have a significant effect. Further, our results in Fig. 3 *c* show that although the deposited particles have similar total surface area, the effect only occurs with the deposition of 20-nm particles. These results provide strong evidence that total available surface area is not responsible for the change in phase behavior of the lung surfactant.

There are at least two other ways in which particle size may impact the isotherm behavior:

1. We note that all of the particles exhibit some degree of aggregation. These are the substantially brighter dots in the images. The aggregates may be the controlling element that interacts with the monolayer to disrupt the phase behavior. To produce a size effect similar to what we observe, this would require that the details of the aggregation be size-dependent. This would essentially be an indirect mechanism in which the particle size produces aggregates that interact with the monolayer in different ways. This could also be connected with a surface area effect if the different size particles produce aggregates with differentiated surface areas based on particle size. Further work would be required to identify the mechanism by which aggregates disrupted the isotherm.
2. Another possibility is that particles of specific size interact directly with specific molecular components of the monolayer in a way that disrupts the squeeze-out behavior. This mechanism is based on reports that the formation of reservoirs in the squeeze-out phase is highly correlated with the associated proteins in the lung surfactant (8–12,14,15,18), and the lack of the surfactant proteins directly enhances the irreversibility of the surfactant films (7). Therefore, it is possible that the deposited 20-nm particles alter the interaction between surfactant proteins and phospholipids. The idea is similar to the behavior observed for the case of hydrophobic, alkylated, gold 2-nm nanoparticles on Survanta. Work on this system shows that particles accumulate with the proteins in the LE phase around the LC domains (36). We suggest a similar interaction in our system where a strong interaction between the small carboxylate-modified charged particles and the surfactant proteins comprises the main factor in the particle-size effect.

It has been reported that the relative lengths of the surfactant proteins are ~2 and 4 nm for hydrophobic SP-C and SP-B, and 20 and 92 nm for hydrophilic SP-A and SP-D (13,17,18). In particular, the initial formation of the reservoirs in the squeeze-out phase requires the presence of SP-B and SP-C to interact with phospholipids (10). For the larger-size particles, the proteins prefer to interact with the surfactant films due to the relatively flat surface curvature of the larger particles. It leads to the normal domain-forming process similar to that for the pure lung surfactant. On the other hand, when the particle sizes are sufficiently small, the surfactant proteins tend to directly interact with the deposited particles. It worth noting that the main squeeze-out-related surfactant protein in Survanta is SP-C.

One possible interaction is that SP-C attaches to the deposited particles by the positive charged N-terminal segment, which is similar to the situation in which the surfactant proteins attach to the small phospholipids bilayer reservoirs (10,56). This process consecutively decreases the active surfactant proteins in the surfactant films under the compression and expansion cycles, which is consistent with the factor that the elimination of the squeeze-out phase gradually appears with the compression cycles. In addition, it also enhances the irregular coalescence of the LC solid phase under compression (7,20,53), resulting in the formation of the networklike LC domains. As with the particle aggregate mechanism, additional work would be needed to determine whether the small particles preferentially interact with the components of the lung surfactant. Furthermore, it is also possible that the effects are a combination of aggregates and individual particles impacting the phase behavior.

In summary, we have provided the experimental evidence for the particle size playing a key role in determining the surfactant phase behavior. It remains an open question whether or not this is a surface area effect driven by differential aggregation of particles or a particle-molecule interaction. Both scenarios are interesting, and the actual mechanism may be a combination of these effects, or another process completely. These issues will be the subject of future studies with other techniques, such as utilizing a single molecule fluorescent microscope to detect the interaction and using an atomic force microscope to study the heterogeneous distribution of the LC domains.

We acknowledge the support of National Science Foundation grant No. NSF-DMR-1309402 and the Research Corporation.

REFERENCES

1. Zasadzinski, J. A., J. Ding, …, A. Waring. 2001. The physics and physiology of lung surfactants. *Curr. Opin. Colloid In.* 6:506–513.
2. Alonso, C., T. Alig, …, J. A. Zasadzinski. 2004. More than a monolayer: relating lung surfactant structure and mechanics to composition. *Biophys. J.* 87:4188–4202.
3. Hills, B. A. 1999. An alternative view of the role(s) of surfactant and the alveolar model. *J. Appl. Physiol.* 87:1567–1583.
4. Avery, M. E., and J. Mead. 1959. Surface properties in relation to atelectasis and hyaline membrane disease. *AMA J. Dis. Child.* 97:517–523.
5. Kaganer, V., H. Möhwald, and P. Dutta. 1999. Structure and phase transitions in Langmuir monolayers. *Rev. Mod. Phys.* 71:779–819.
6. Casals, C., and O. Cañadas. 2012. Role of lipid ordered/disordered phase coexistence in pulmonary surfactant function. *Biochim. Biophys. Acta.* 1818:2550–2562.
7. Ding, J., D. Y. Takamoto, …, J. A. Zasadzinski. 2001. Effects of lung surfactant proteins, SP-B and SP-C, and palmitic acid on monolayer stability. *Biophys. J.* 80:2262–2272.
8. Cruz, A., L. Vázquez, …, J. Pérez-Gil. 2004. Effect of pulmonary surfactant protein SP-B on the micro- and nanostructure of phospholipid films. *Biophys. J.* 86:308–320.
9. Serrano, A. G., and J. Pérez-Gil. 2006. Protein-lipid interactions and surface activity in the pulmonary surfactant system. *Chem. Phys. Lipids.* 141:105–118.
10. Pérez-Gil, J. 2008. Structure of pulmonary surfactant membranes and films: the role of proteins and lipid-protein interactions. *Biochim. Biophys. Acta.* 1778:1676–1695.
11. Pérez-Gil, J., and K. M. W. Keough. 1998. Interfacial properties of surfactant proteins. *Biochim. Biophys. Acta Mol. Basis. Dis.* 1408:203–217.

12. Krol, S., M. Ross, …, A. Janshoff. 2000. Formation of three-dimensional protein-lipid aggregates in monolayer films induced by surfactant protein B. *Biophys. J.* 79:904–918.

13. Haagsman, H. P., and R. V. Diemel. 2001. Surfactant-associated proteins: functions and structural variation. *Comp. Biochem. Physiol. A Mol. Integr. Physiol.* 129:91–108.

14. Veldhuizen, E. J., and H. P. Haagsman. 2000. Role of pulmonary surfactant components in surface film formation and dynamics. *Biochim. Biophys. Acta.* 1467:255–270.

15. Galla, H. J., N. Bourdos, …, M. Sieber. 1998. The role of pulmonary surfactant protein C during the breathing cycle. *Thin Solid Films.* 327–329:632–635.

16. Hawgood, S., M. Derrick, and F. Poulain. 1998. Structure and properties of surfactant protein B. *Biochim. Biophys. Acta Mol. Basis. Dis.* 1408:150–160.

17. Johansson, J. 1998. Structure and properties of surfactant protein C. *Biochim. Biophys. Acta Mol. Basis. Dis.* 1408:161–172.

18. Frey, S. L., L. Pocivavsek, …, K. Y. Lee. 2010. Functional importance of the NH2-terminal insertion sequence of lung surfactant protein B. *Am. J. Physiol. Lung C.* 298:L335–L347.

19. Nag, K., J. Perez-Gil, …, K. M. Keough. 1998. Phase transitions in films of lung surfactant at the air-water interface. *Biophys. J.* 74:2983–2995.

20. Keating, E., Y. Y. Zuo, …, R. A. W. Veldhuizen. 2012. A modified squeeze-out mechanism for generating high surface pressures with pulmonary surfactant. *Biochim. Biophys. Acta.* 1818:1225–1234.

21. Piknova, B., V. Schram, and S. B. Hall. 2002. Pulmonary surfactant: phase behavior and function. *Curr. Opin. Struct. Biol.* 12:487–494.

22. Baoukina, S., L. Monticelli, …, D. P. Tieleman. 2008. The molecular mechanism of lipid monolayer collapse. *Proc. Natl. Acad. Sci. USA.* 105:10803–10808.

23. Lee, K. Y. 2008. Collapse mechanisms of Langmuir monolayers. *Annu. Rev. Phys. Chem.* 59:771–791.

24. Goto, T. E., and L. Caseli. 2013. Understanding the collapse mechanism in Langmuir monolayers through polarization modulation-infrared reflection absorption spectroscopy. *Langmuir.* 29:9063–9071.

25. Xiong, S., S. George, …, J. S. Loo. 2013. Size influences the cytotoxicity of poly (lactic-co-glycolic acid) (PLGA) and titanium dioxide (TiO_2) nanoparticles. *Arch. Toxicol.* 87:1075–1086.

26. Schleh, C., C. Mühlfeld, …, J. M. Hohlfeld. 2009. The effect of titanium dioxide nanoparticles on pulmonary surfactant function and ultrastructure. *Respir. Res.* 10:90.

27. Zhao, X., S. Ng, …, S. C. Loo. 2013. Cytotoxicity of hydroxyapatite nanoparticles is shape- and cell-dependent. *Arch. Toxicol.* 87:1037–1052.

28. Li, N., C. Sioutas, …, A. Nel. 2003. Ultrafine particulate pollutants induce oxidative stress and mitochondrial damage. *Environ. Health Perspect.* 111:455–460.

29. Fan, Q., Y. E. Wang, …, Y. Y. Zuo. 2011. Adverse biophysical effects of hydroxyapatite nanoparticles on natural pulmonary surfactant. *ACS Nano.* 5:6410–6416.

30. Beck-Broichsitter, M., C. Ruppert, …, T. Gessler. 2011. Biophysical investigation of pulmonary surfactant surface properties upon contact with polymeric nanoparticles in vitro. *Nanomedicine (Lond. Print).* 7:341–350.

31. Samet, J. M., F. Dominici, …, S. L. Zeger. 2000. Fine particulate air pollution and mortality in 20 U.S. cities, 1987–1994. *N. Engl. J. Med.* 343:1742–1749.

32. Guzmán, E., L. Liggieri, …, F. Ravera. 2013. Mixed DPPC-cholesterol Langmuir monolayers in presence of hydrophilic silica nanoparticles. *Colloids Surf. B Biointerfaces.* 105:284–293.

33. Guzmán, E., L. Liggieri, …, F. Ravera. 2012. Influence of silica nanoparticles on phase behavior and structural properties of DPPC–palmitic acid Langmuir monolayers. *Colloid. Surface. A.* 413:280–287.

34. Mühlfeld, C., B. Rothen-Rutishauser, …, P. Gehr. 2008. Interactions of nanoparticles with pulmonary structures and cellular responses. *Am. J. Physiol. Lung C.* 294:L817–L829.

35. Harishchandra, R. K., M. Saleem, and H.-J. Galla. 2010. Nanoparticle interaction with model lung surfactant monolayers. *J. R. Soc. Interface.* 7:S15–S26.

36. Tatur, S., and A. Badia. 2012. Influence of hydrophobic alkylated gold nanoparticles on the phase behavior of monolayers of DPPC and clinical lung surfactant. *Langmuir.* 28:628–639.

37. Farnoud, A. M., and J. Fiegel. 2013. Interaction of dipalmitoyl phosphatidylcholine monolayers with a particle-laden subphase. *J. Phys. Chem. B.* 117:12124–12134.

38. Farnoud, A. M., and J. Fiegel. 2012. Low concentrations of negatively charged sub-micron particles alter the microstructure of DPPC at the air–water interface. *Colloid. Surface. A.* 415:320–327.

39. Bakshi, M. S., L. Zhao, …, N. O. Petersen. 2008. Metal nanoparticle pollutants interfere with pulmonary surfactant function in vitro. *Biophys. J.* 94:855–868.

40. Dwivedi, M. V., R. K. Harishchandra, …, H.-J. Galla. 2014. Size influences the effect of hydrophobic nanoparticles on lung surfactant model systems. *Biophys. J.* 106:289–298.

41. Li, N., M. Hao, …, A. E. Nel. 2003. Particulate air pollutants and asthma. A paradigm for the role of oxidative stress in PM-induced adverse health effects. *Clin. Immunol.* 109:250–265.

42. Oberdorster, G., R. M. Gelein, …, B. Weiss. 1995. Association of particulate air pollution and acute mortality: involvement of ultrafine particles? *Inhal. Toxicol.* 7:111–124.

43. Kapp, N., W. Kreyling, …, M. Geiser. 2004. Electron energy loss spectroscopy for analysis of inhaled ultrafine particles in rat lungs. *Microsc. Res. Tech.* 63:298–305.

44. Geiser, M., B. Rothen-Rutishauser, …, P. Gehr. 2005. Ultrafine particles cross cellular membranes by nonphagocytic mechanisms in lungs and in cultured cells. *Environ. Health Perspect.* 113:1555–1560.

45. Kreyling, W. G., M. Semmler-Behnke, and W. Möller. 2006. Ultrafine particle-lung interactions: does size matter? *J. Aerosol Med.* 19:74–83.

46. Pope, 3rd, C. A., R. T. Burnett, …, G. D. Thurston. 2002. Lung cancer, cardiopulmonary mortality, and long-term exposure to fine particulate air pollution. *JAMA.* 287:1132–1141.

47. Sachan, A. K., R. K. Harishchandra, …, H.-J. Galla. 2012. High-resolution investigation of nanoparticle interaction with a model pulmonary surfactant monolayer. *ACS Nano.* 6:1677–1687.

48. Reference deleted in proof.

49. Kuo, C.-C., A. T. Kodama, …, M. Dennin. 2012. Particle size effects on collapse in monolayers. *Langmuir.* 28:13976–13983.

50. McConnell, H. M. 1991. Structures and transitions in lipid monolayers at the air-water interface. *Annu. Rev. Phys. Chem.* 42:171–195.

51. Discher, B. M., W. R. Schief, …, S. B. Hall. 1999. Phase separation in monolayers of pulmonary surfactant phospholipids at the air-water interface: composition and structure. *Biophys. J.* 77:2051–2061.

52. Jiao, X., E. Keating, …, R. A. W. Veldhuizen. 2011. Atomic force microscopy analysis of rat pulmonary surfactant films. *Biophys. Chem.* 158:119–125.

53. Dhar, P., E. Eck, …, J. A. Zasadzinski. 2012. Lipid-protein interactions alter line tensions and domain size distributions in lung surfactant monolayers. *Biophys. J.* 102:56–65.

54. Oberdörster, G., E. Oberdörster, and J. Oberdörster. 2005. Nanotoxicology: an emerging discipline evolving from studies of ultrafine particles. *Environ. Health Perspect.* 113:823–839.

55. Sirsi, S. R., C. Fung, …, M. A. Borden. 2013. Lung surfactant microbubbles increase lipophilic drug payload for ultrasound-targeted delivery. *Theranostics.* 3:409–419.

56. Baoukina, S., and D. P. Tieleman. 2011. Lung surfactant protein SP-B promotes formation of bilayer reservoirs from monolayer and lipid transfer between the interface and subphase. *Biophys. J.* 100:1678–1687.